

Estimation of Rice Yield Considering Heading Stage Using Satellite Imagery and Ground-Based Data in Indonesia

Yuki Sofue¹, Chiharu Hongo¹, Naohiro Manago¹, Gunardi Sigit², Koki Homma³ & Budi Utoyo²

¹ Center for Environmental Remote Sensing, Chiba University, Chiba, Japan

² Regional Office of Food Crops Service West Java Province, Indonesia

³ Tohoku University, Miyagi, Japan

Correspondence: Yuki Sofue, Center for Environmental Remote Sensing, Chiba University, 1-33, Yayoicho, Inageku, Chiba City, Chiba Prefecture, Japan. Tel: 81-43-290-3021. E-mail: yuki.candy.s126@chiba-u.jp

Received: May 24, 2022

Accepted: June 28, 2022

Online Published: July 15, 2022

doi:10.5539/jas.v14n8p1

URL: <https://doi.org/10.5539/jas.v14n8p1>

The research is financed by a program of SATREPS (Science and Technology Research Partnership for Sustainable Development) [Grant Number: JPMJSA1604].

Abstract

Understanding the temporal and spatial variability in crop yield is considered as one of the key steps in agricultural risk assessment. Therefore, a study of an irrigated area in Cihea, West Java, Indonesia, was conducted to assess rice yield per field using SENTINEL-2 imagery and yield observation data in 2018 and 2019. The study area is located in the Citarum River basin. SENTINEL-2 images were used to derive paddy rice's growth curve and estimate rice growth stages based on the normalized difference vegetation index. Using these results, the regression model formula using Band 4 (665 nm) and the normalized difference water index in the ripening stage was created ($R^2 = 0.40$, RMSE = 1.21 t/ha). The results from this model were used to generate yield maps, which illustrated a distinct spatial variation in rice yield, such as the average rice productivity in the study area was relatively high, however, the difference between years tended to be small in the upper stream area. The results of this study show that this method is effective in this area to monitor rice yield condition and distribution.

Keywords: growth stage, paddy rice, SENTINEL-2, vegetation index

1. Introduction

Small farmers around the world face many risks that threaten income stability, such as pests and diseases, extreme weather conditions, and so on (O'Brien et al., 2004). These risks are further increased by the impacts of climate change, such as changes in rainfall distribution increased frequency, and duration of extreme weather events such as droughts and floods, among which tropical countries are the most vulnerable regions to these impacts (Morton, 2007). In monsoon Asia, the increase in food demand by rapid population growth is remarkable. Rice is one of the major foods in this region, and it has been pointed out that there are two possible patterns of response in terms of yield, a decrease in rice yield due to an increase in temperature, a decrease in solar radiation, and a change in precipitation, and an increase in yield due to an increase in photosynthesis because of an increase in carbon dioxide concentration (Song et al., 2022; Franks et al., 2013; Ainsworth, 2008). Indonesia is one of the countries that has been reported to be strongly influenced by the interannual variability of precipitation in agriculture due to the Asia-Australia monsoon and the El Nino Southern Oscillation (ENSO) (Hackert & Hastenrath, 1986). One previous study indicates that the dry season was clearly extended because the wet season was delayed in the ENSO year (Naylor, Battisti, Vimont, Falcon, & Burke, 2007). To reduce the risk of crop damage due to climate change, agricultural insurance is one of the effective tools to prevent the income decline of farmers and mitigate food safety problems (Miranda & Gonzalez-Vega, 2011), and it is essential to develop a method for quantitative damage assessment (Hongo, Tsuzawa, Tokui, & Tamura, 2015).

In the world, a variety of damage assessment methods for calculating agricultural insurance payments have been tried and implemented by the government (Mahul & Stutley, 2010). For instance, Weather Index Insurance is an insurance system that works when rainfall records below a certain threshold based on evaluation indices such as

rainfall observed by weather stations or satellites in each region (Kuwata, Mahmood, & Shibasaki, 2015). However, it has been pointed out that the gap between the actual damage and the evaluation result by the measured value of the index is a serious problem as a basis risk (Doherty & Richter, 2002). In the case of Japan, the average yield is the yield per 1,000 m² (= 10 are) estimated before the cultivation of paddy rice is started based on the actual yield data of the past, when the weather change in the year and the weather damage such as low temperature and sunshine shortage are considered to be average, and it is regarded as the standard of the crop condition index which indicates the quality of the yield. In Japan, the actual yield data have been stocked, and the average yield has been calculated using the yield data per field. The data has been corrected by the AMeDAS data since 1979 when the meteorological observation system was arranged. In Japan's Agricultural Insurance Scheme (called as NOSAI), this is used as a standard yield for the insurance payment.

On the other hand, one of the current evaluation methods in the agricultural insurance system in Indonesia is a visual interpretation of diseases and pests, droughts, etc. by pest observers in field surveys. In the current evaluation system, the pest observers must visit each field, observe paddy conditions, and the insurance money is paid when the damage to paddy rice by disease or insect damage is judged to reach over a certain rate value of the field. The addition of a yield-based evaluation method can make the gap between the evaluation of damage and actual damage less and lead to a more quantitative evaluation of damages. However, in Indonesia, there is no accumulation of observed yield data and there are many data that are difficult to obtain such as data on climate, fertilizer type, and agricultural chemicals data. Therefore, it takes a great deal of labor, time, and cost to collect these data. A remote sensing technique using satellite data is an effective tool to reduce these burdens. In agriculture, the prediction of crop yield and its spatial pattern is widely carried out by relating the characteristics of the spectrum and vegetation index (VI) calculated from the reflectance extracted from satellite images with the plant physics viewpoint (Chen, Quilang, Alosnos, & Finnigan, 2011). In recent years, crop yield estimation using SENTINEL-2 satellite data with high spatial and temporal resolution has been widely carried out and used for rice yield estimation (Soriano-González, Angelats, Martínez-Eixarch, & Alcaraz, 2022). The remote sensing data obtained from such satellite data can be used as spatial information for agricultural monitoring that reflects the effects of the growing environment of crops, including weather and land conditions (Liu & Kogan, 2002). Therefore, even when it is difficult to obtain such information as observed yield, meteorological data such as temperature and precipitation in the study area, and other information such as the amount and type of fertilizer applied, the spectral information obtained from the satellite data is considered to represent these differences.

Rice yield estimation using remote sensing techniques is carried out all over the world, but the research conducted in the agricultural environment of Indonesia is still limited, and it is necessary to examine the estimation technique suitable for this region. In Indonesia, the size of fields is irregular and fields of various growth stages are intermingled because the planting date is different by the area. For these reasons, in Indonesia, the analysis technique considering the growth stage of each field is essential, and there are few reports on the yield estimation using the technique considering this point. Therefore, the purpose of this study is to extract the growth curve in each field based on the heading stage, examine the possibility of yield estimation using wavelength and index for each growth stage, and understand the spatial distribution of productivity in the field unit.

2. Method

2.1 Study Area

West Java has the highest rice production in Indonesia and the largest paddy field area in the country. However, a comparison of the yield per hectare in West Java shows that the yield is about 5.2 t/ha, which is lower than that of Bali (5.59 t/ha), East Java (5.34 t/ha), and Central Java (5.23 t/ha) (Panuju, Mizuno, & Trisasongko, 2013). The study area is the irrigated area in Cihea (6°50'S, 107°16'E) located in the northeast of Cianjur, West Java, Indonesia. This region is one of the main rice production regions in West Java, and the dry season is from June to September and the rainy season is from December to March. This study area is in the Citarum river basin, and the north side is the lower stream area and the south side is the upper stream area. Here, paddy rice is transplanted mainly two or three times per year. The first transplanting is the rainy season from October to April, the second is the dry season from May to August, and the third is the second dry season from August to October. In this study, the dry season corresponding to the second season of transplanting was analyzed. In the study area, the test site (About 250 ha) has been set as one of the SATREPS project activities, and about 6000 fields are included. For these fields, polygons for each field have been created as the test site field. In the test site field, there is data on the rice variety for each area, and it is possible to know the variety cultivated in the target period. Figure 1 shows the location of the entire area and the test site.

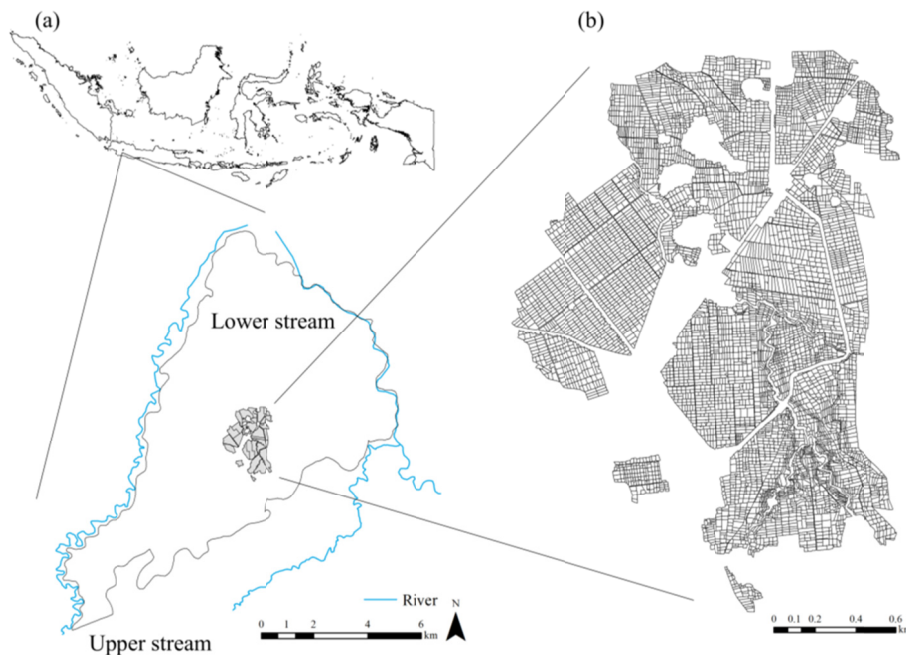


Figure 1. Locations of (a); study area and (b); test site in the study area

2.2 Ground-Based Data

Yield investigation was carried out in the study area from July 16 in 2018 to 18, from August 1 to 3, and from August 11 in 2019 to 23 in the harvesting stage. The number of fields used for this analysis was 38 in 2018 and 59 in 2019, for a total of 97 fields. In each field, two plots were set on a diagonal line, and a total of nine rice plants (3×3 plants per plot) were harvested as samples, and the distance between each plant was measured with a folding ruler. The yield per hectare (t/ha) was calculated using these field data. Yields in each year were approximately 6~10 t/ha (Figure 2). The survey sites with measured yields less than 4t/ha were located in the lower stream area, and drought damage was observed during the field investigation. And in the investigation, the hearing survey for transplanting date and variety was also carried out for the farmers.

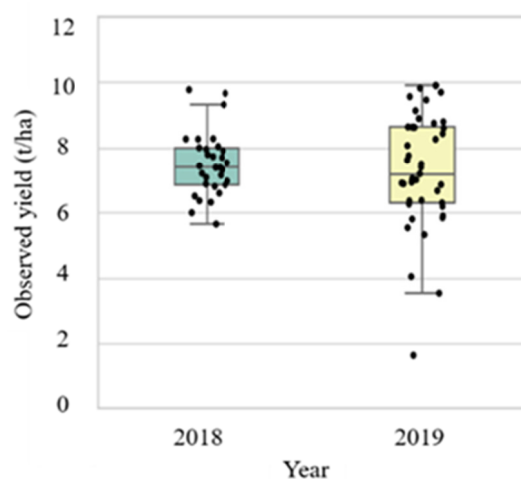


Figure 2. Observation yield of 2018 and 2019

2.3 Satellite Imagery

2.3.1 SENTINEL-2 Data

For the satellite image of the study area in 2018, bands 2 to 12 in the Level-1 C (L1C) product of SENTINEL-2 satellite data developed by ESA were used. For the atmospheric correction of the satellite image data, the SEN2COR plug-in of Sentinel Applications Platform (SNAP) developed and released by ESA was used, and the terrain correction processing was performed using SRTM DEM. For the satellite image in 2019, SENTINEL-2 satellite data were used the same as in 2018, but bands 2 to 12 in the Level-2A (L2A) product were used because the L2A products, on which atmospheric correction had already been done, were available. Since the L2A product is based on the L1C and atmospheric correction was performed through the SEN2COR plug-in, the data used in this analysis between 2018 and 2019 were used as if there were no differences due to atmospheric correction processing. A summary of the SENTINEL-2 satellite data is shown in Table 1. The study period of the field investigation was mainly from April to May in both years. Considering that the transplanting period varies depending on the field, we obtained SENTINEL-2 satellite data from January to September of each year. The data were preprocessed including geometric correction, resampling, and cropping of the study area. The spatial resolution of the band for each wavelength is different from 10 m, 20 m, and 60 m, respectively, and here, and resampled with 10m grid. Using the Scene Classification (SC) band in the product, pixel values classified into clouds and shadows were excluded. And, the image in which the cloud covers the whole study area and the correction is difficult was excluded.

Table 1. Description of SENTINEL-2 satellite data and calculated indices in this analysis

SENTINEL-2	
Resolution	10/20/60 m
Band (Central Wavelength)	Band 1 (443 nm)
	Band 2 (490 nm)
	Band 3 (560 nm)
	Band 4 (665 nm)
	Band 5 (705 nm)
	Band 6 (740 nm)
	Band 7 (783 nm)
	Band 8 (842 nm)
	Band 8a (865 nm)
	Band 9 (946 nm)
	Band 10 (1374 nm)
	Band 11 (1610 nm)
Band 12 (2190 nm)	

2.3.2 Precipitation Data

Global Rainfall Map (GSMaP) by JAXA Global Rainfall Watch' was produced and distributed by the Earth Observation Research Center, Japan Aerospace Exploration Agency (Kubota et al., 2020). It incorporates both passive microwave (PMW) and infrared (IR) sensors data from the satellite to map global precipitation at high temporal and spatial resolution. In this study, MVK standard product version 7 was used as precipitation data. They offer hourly precipitation estimates on 0.1° latitude/longitude grid over the globe (60°S to 60°N) from March 2014 to the present. We extracted 3 × 3 pixels around the study area and calculated the average values in 2018 and 2019. Figure 3 showed the daily mean of the precipitation change during the rice growth season in 2018 and 2019.

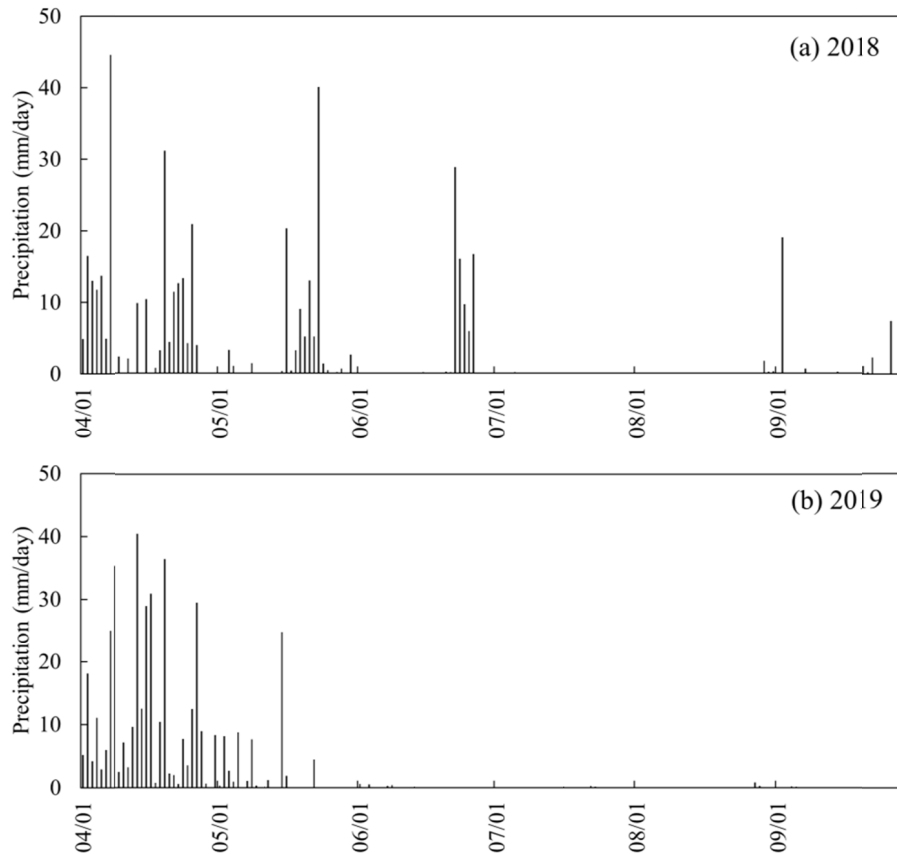


Figure 3. Daily mean precipitation in (a): 2018 and (b): 2019

2.3.3 Solar Radiation Data

The limiting factors of plants are generally water conditions and energy conditions such as temperature and solar radiation (Swami, 2017). In Indonesia, the irrigated rice crop fields have less impact on rice yield of temperature rise compared with rainfed fields (Yuliawan & Handoko, 2016). Here, therefore, we confirmed solar radiation conditions in each upper stream area and lower stream area. AMATERASS solar radiation data were used in this analysis. AMATERASS solar radiation dataset is developed based on the Advanced Himawari Imagers (AHIs) aboard Himawari-8 acquire full-disk observations in 16 observation bands (three for visible, three for near infrared, and 10 for infrared wavelengths) every 10 min, with a spatial resolution ranging from 0.5 to 2 km (Bessho et al., 2016; Takenaka et al., 2011). The algorithm is based on a fast neural network, accurately reproducing the radiative transfer model. The surface downwelling solar radiation data were used as solar radiation data for this study area. The spatial resolution is 4 km. Here, eight pixels covering the study area were extracted and divided into three categories: the top two pixels are upper stream, the middle five are middle stream and the bottom one is a lower stream, and the daily average solar radiation for each pixel in each stream area was calculated from the data every 10 minutes. Figure 4 showed the simple moving average of daily mean solar radiation in 2018 and 2019 according to three watersheds. Also, the difference of a simple moving average of daily mean solar radiation between each watershed in 2018 and 2019 was shown in Figure 5. In Figure 5, positive values showed that solar radiation in the lower stream was higher than in the upper stream (Figure 5(a)) and that in the middle stream higher than in the upper stream (Figure 5(b)). Negative values in these figures mean the opposite.

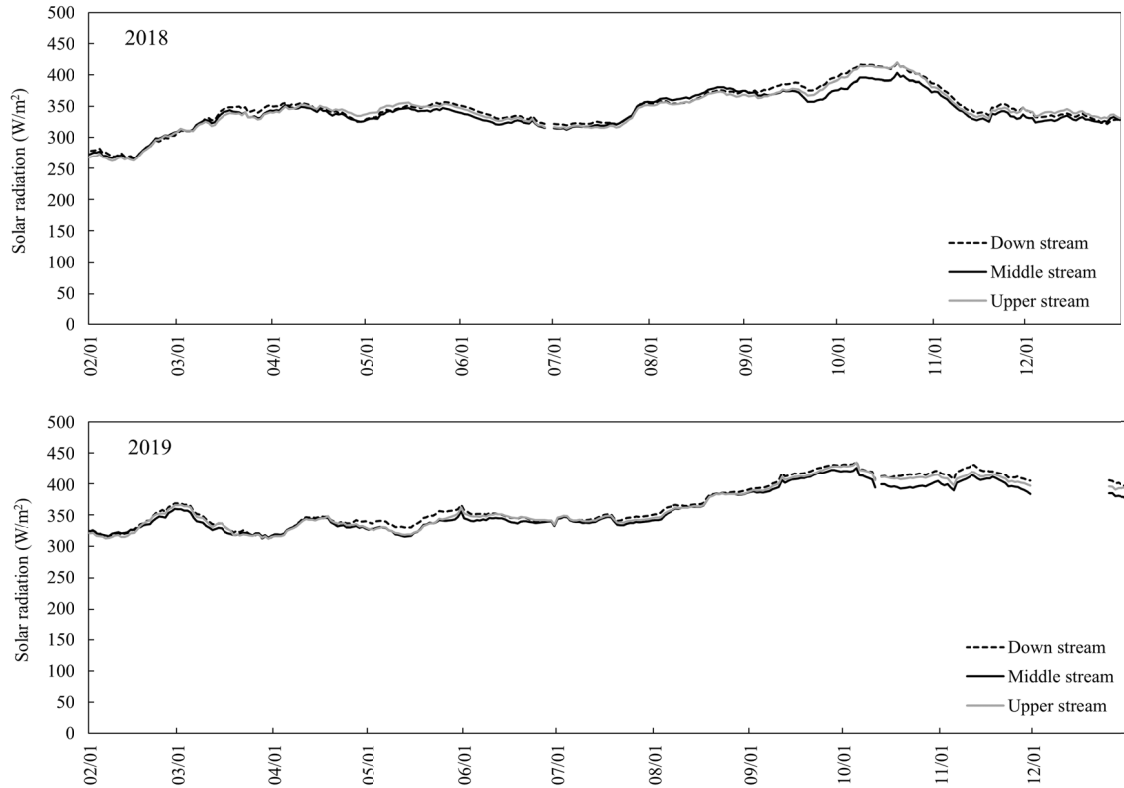


Figure 4. Simple moving average of daily mean solar radiation in 2018 and 2019

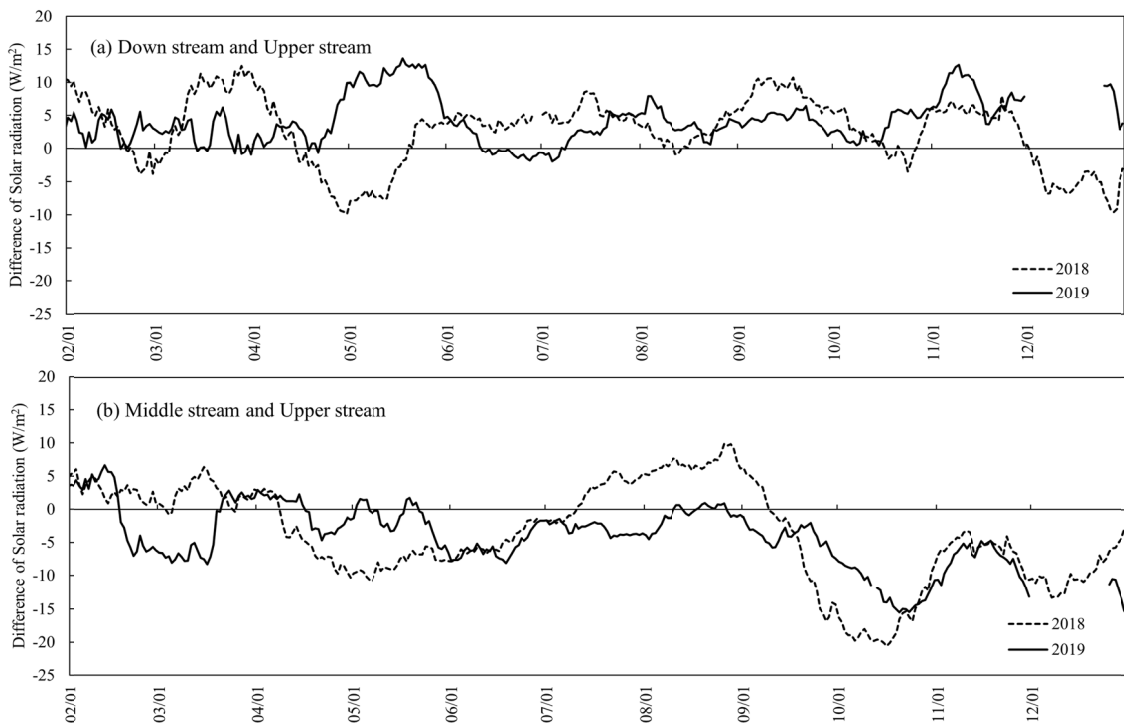


Figure 5. Difference of simple moving average of daily mean solar radiation in 2018 and 2019. (a) Difference between the lower stream and the upper stream; (b) Difference between the middle stream and the upper stream

2.4 Methods

The preprocessed data were used to calculate the normalized difference vegetation index (NDVI) and the normalized difference water index (NDWI). The calculations for each index are given in Equations 1 and 2.

$$NDVI = (NIR - Red) / (NIR + Red) \quad (1)$$

$$NDWI = (NIR - SWIR) / (NIR + SWIR) \quad (2)$$

Band 4 was applied to Red, Band 8 to NIR, and Band 11 to SWIR in (1) and (2). The NDWI used here was established to estimate water content in plants (Gao, 1996). Gao (1996) used the 1.24 μm in a weak absorption band of water as SWIR. Among the observed wavelength bands of SENTINEL-2, band 11 (1.61 μm) is at the edge of a strong water absorption band, so band 11 is used as SWIR.

The vegetation index represented by NDVI rises with the growth of paddy rice from transplanting, and it starts to decrease after several days from heading as a peak, and the harvest time comes after the ripening period. In this analysis, NDVI was used to estimate the heading stage. Time series NDVI of each pixel of the satellite image was calculated, smoothed out by a cubic smoothing spline to remove noise (Boor, 1978), and interpolated to obtain daily data. Then, the time when NDVI took the maximum value in the period from 30 days to less than 100 days from the transplanting date was defined as the heading stage. Smoothed NDVI of a paddy field was shown in Figure 6 as an example. The green line of this figure shows the transplanting date. Extraction of paddy fields and estimation of transplanting dates have already been carried out based on Sentinel-1 (Manago, Hongo, Sofue, Sigit, & Utoyo, 2020). The paddy field distribution and transplanting dates used in this analysis are based on the results. Also, the result of a hearing survey of transplanting date was used in addition to the estimation result by the previous study.

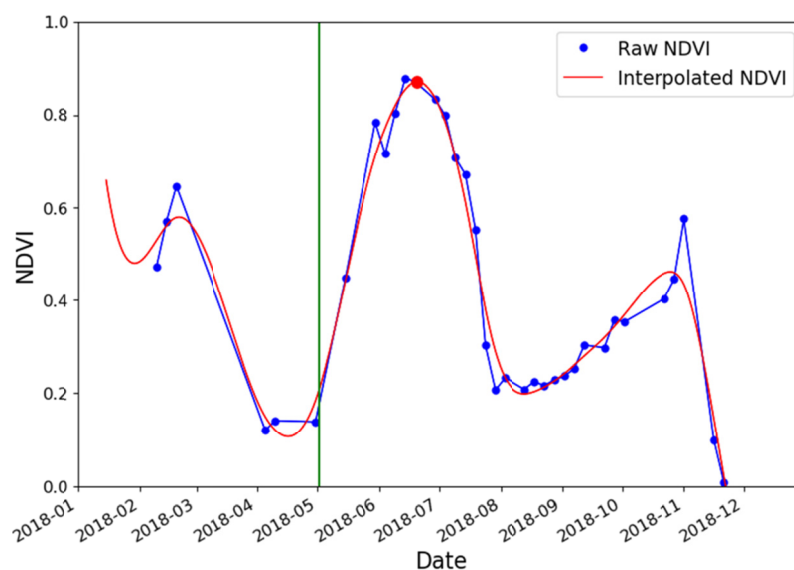


Figure 6. Spline smoothing of time series NDVI of rice growth season

In previous studies, it is clarified that the rice yield has a high relationship with NDVI at the heading stage and NDVI after the stage respectively (Liu et al., 2015), while some reports pointed out that it is highly related to the spectral reflectance of rice at the booting stage and ripening stage (Kawamura, Ikeura, Phongchanmaixay, & Khanthavong, 2018; Moseleh, Hassan, & Chowdhury, 2016). These differences are considered to be due to environmental factors in the study area and differences in rice varieties. Based on these previous studies, this analysis included the period from the heading period estimated by time series NDVI to 40 days every 5 days. Each reflectance from band 2 to band 12 in each period was extracted, and VIF (Variance Inflation Factor) was calculated to remove the band which could become multiple collinear. VIF is expressed by the following formula.

$$VIF = \frac{1}{(1 - R^2)} \quad (3)$$

Generally, the multiple collinearity is suspected, when the VIF is over 10. Then, in this analysis, the regression model using the data of every 5 days was made using the wavelength band in which VIF showed values less than 10. The VIF between each band is shown in Table 2.

In the model preparation, the parameter was chosen considering AIC (Akaike Information Criterion) (Akaike, 1998). The AIC is defined by the following equation.

$$AIC = n \left[\log \left(2\pi \frac{S_e}{n} \right) + 1 \right] + 2(p + 2) \quad (4)$$

where, n is a sample size, p is the number of explanatory variables, S_e is the residual sum of squares, and the log is the natural logarithm. The accuracy of each model was verified using five-fold cross-validation by random data partitioning. The model equation chosen based on the AIC, RMSE, and coefficient of determination is shown in Equation (5). The accuracies of other equations are shown in Table 3. The parameters selected for the equation with the best accuracy were band4 and NDWI at 25 days after the estimated heading stage.

$$Y = 122.97 \cdot \text{Red} + 21.96 \cdot \text{NDWI} - 6.32 \quad (5)$$

For the fields in the test site, the analysis using the above technique was conducted using the weighted average value of each pixel value contained in each field. A pixel-based analysis was performed in the area outside the test sites.

Table 2. VIF values between the parameters (* shows VIFs above 10)

VIF	Band											
	2	3	4	5	6	7	8	9	11	12	NDVI	
3	3.45											
4	1.82	1.96										
5	1.90	3.10	2.05									
6	1.06	1.00	1.65	1.01								
7	1.14	1.02	2.14	1.10	22.31*							
8	1.08	1.01	1.93	1.06	11.15*	17.21*						
9	1.13	1.02	2.05	1.09	19.15*	131.10*	15.99*					
11	1.51	1.85	1.59	3.44	1.01	1.06	1.03	1.07				
12	1.48	1.50	1.84	2.87	1.13	1.28	1.19	1.29	7.99			
NDVI	1.08	1.01	1.93	1.06	11.15*	17.21*	833.33*	15.99*	1.03	1.19		
NDWI	1.51	1.85	1.59	3.44	1.01	1.06	1.03	1.07	8326.33*	7.99	1.03	

Table 3. The accuracies of all models on each number of days from the estimated heading stage. Values in the table are coefficients of determination (R^2), RMSE, and AIC

	Number of days after heading stage									
	0	5	10	15	20	25	30	35	40	
R^2	0.212	0.23	0.29	0.32	0.35	0.40	0.39	0.28	0.13	
RMSE (t/ha)	1.38	1.38	1.32	1.28	1.26	1.21	1.22	1.34	1.46	
AIC	298.3	297.3	292.7	288.5	283.4	276.7	278.0	293.5	308.9	

3. Results and Discussion

3.1 Creation of a Yield Estimation Model Using Growth Curves

Among the periods from heading to 40 days after heading, the yield estimation error tended to be smallest in the period corresponding to 25 days (Table 3). This period corresponds to the ripening stage in the growth period of paddy rice, and the effect of the environment in this period on the yield is indicated. For instance, high temperatures during the ripening stage decrease the supply of carbohydrates from the vegetative organs to developing cereals, and yield tends to decrease because accumulation in the unhulled rice is inadequate (Kobata & Uemuki, 2004). In addition, the environment during this period had a significant effect on the yield, as evidenced by a decrease in yield due to water stress during the ripening period (Zaman, Abdullah, Othman, & Zaman, 2018). Therefore, the result of this analysis can be explained by the previous studies. The relationship between the estimated yield that was calculated using Equation 5 and the observed yield is shown in Figure 7,

and the relationship between the observed yield and each parameter is shown in Figure 8. As a result of the 5-fold cross-validation, $R = 0.52$ ($p < 0.05$).

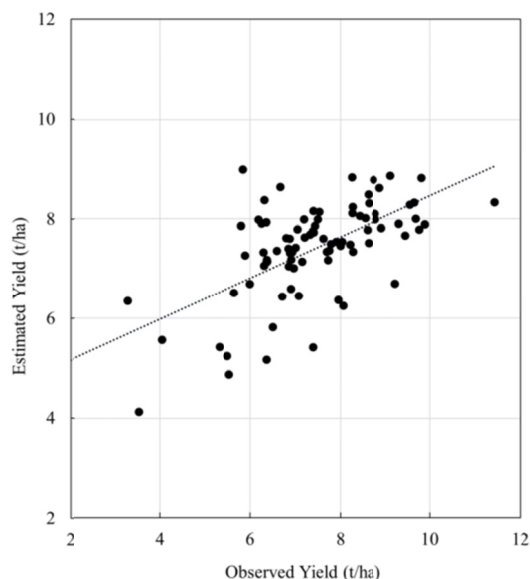


Figure 7. Relationship between observed and estimated yield

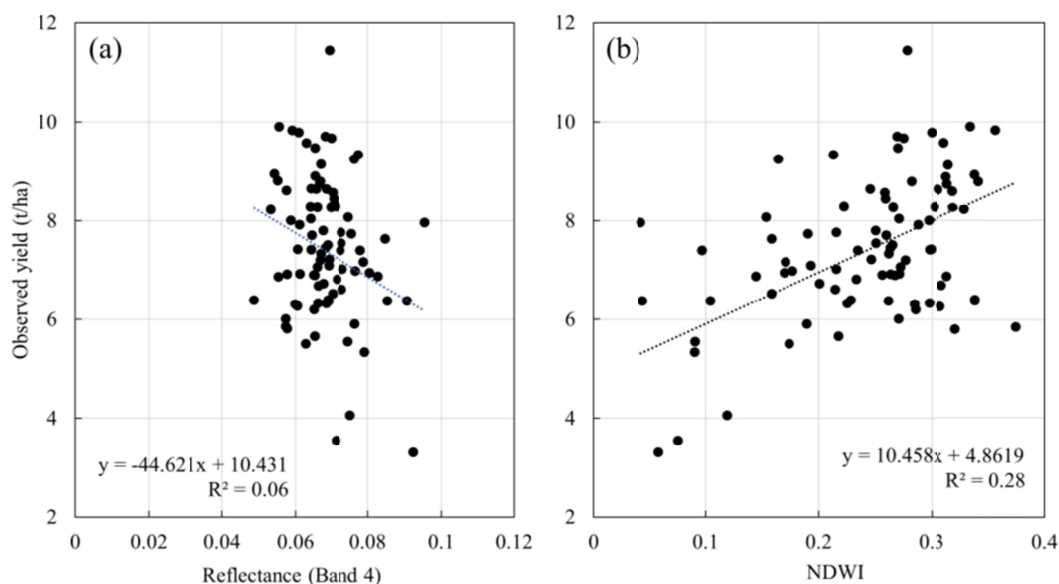


Figure 8. Relationship between each investigated variable and the observed yield. (a); Relationship between Red reflectance (Band4) and observed yield, (b); Relationship between NDWI and observed yield

In a single correlation, the higher the absorption rate of band 4 (665 nm), the higher the estimated yield. In general, the light absorption properties of chlorophyll in plants have peaks at around 430 nm and 662 nm (Du, Fuh, Li, Corkan, & Lindsey, 2008). Therefore, the higher the chlorophyll content, the higher the absorption of band 4 (665 nm).

The tropical region in which Indonesia is located has small temperature differences throughout the year. For the reference, Figure 9 shows the daily mean temperature from April to September 2019 observed by HOBO station near the test site. This figure shows that the daily mean temperature from April to September 2019 varied mainly between 25 °C and 28 °C. According to this temperature variation in this study area, water is expected to be the main limiting factor for rice growth because of the stable high air temperature. Figure 8(b) show that the higher

the NDWI which means water content of rice, the more likely it is to increase the yield. Our results showed that NDWI is one of the dominant factors for rice yield, and that was similar to those reported in JesúsSoriano-González et al. (2022) in rice yield estimation using SENTINEL-2 data.

Here, the correlation coefficient between yield and red alone and the correlation coefficient between yield and red when red and NDWI are combined are different in sign. The results showed a possibility that there is multicollinearity between red and NDWI. Therefore, we calculated the standard error of the regression coefficient for both parameters. The standard error of the regression coefficient of Red is 28.52 and that of NDWI is 3.18. Therefore, it is considered that the regression coefficient of both of them could be reliable.

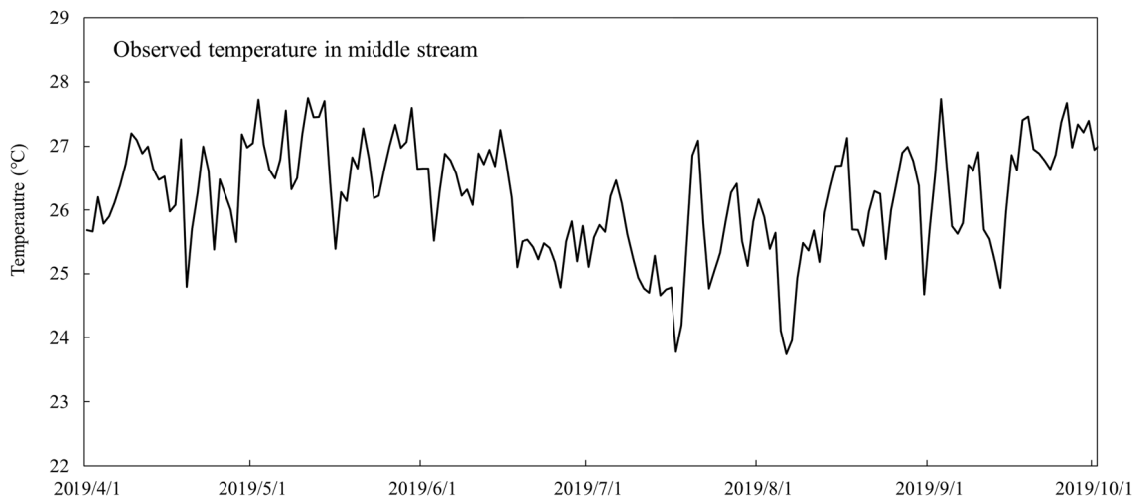


Figure 9. Daily mean temperature from April to September 2019 observed by HOBO station near the test site

3.2 Yield Distribution of the Study Area Based on Average Yield

Figures 10(a) and 10(b) show the distribution of the mean estimated yield values of the whole area and the test sites in Cihea over the two years. In the study period, the yield difference by the region tended to be high a little in the upper stream region, and it tended to be low in the study area tip in the lower stream, but the yield tended to be high in the whole area. Drought damage is observed more frequently in the tip of the study area in the lower stream area than in other areas, and drought is confirmed in the field investigation. These differences are considered to be due to regional differences in climate conditions such as precipitation and solar radiation. For example, Figure 5(a) showed that solar radiation in the lower stream was higher than upper stream area. It can be one cause that drought was susceptible to occur in lower stream areas in the target period. One of the major rice varieties in Indonesia is Ciherang, which is also widely cultivated in the study area. The average yield of this cultivar was reported to be 6 to 8.5 t/ha (Santosa & Suryanto, 2015). Compared with this average yield, the yield of the study area was average or slightly higher.

Figure 10(b) shows that there is a maximum difference of about 3 t/ha in the average yield among the fields. In the study area, the variety which differs by the year is cultivated. Then, in order to confirm whether this difference is the difference by the variety, the time series change of each band and index was confirmed for each field of the variety different. In the comparison between varieties in the test site field, the difference of the time series change by the difference of varieties was not confirmed. This result suggested that the differences observed among the fields are not due to differences in the varieties, but to differences in the environmental conditions.

The test site is not a large area, so that solar radiation is unlikely assumed different between each field. As a country located on the equator, Indonesia is overflowing with rainfall more than enough, but due to a lack of good water management, the Indonesian State water deficit (Yazd, Wheeler, & Zuo, 2020). On the other hand, Sujono (2010) reported that the lower production was affected by the lower number of tillers due to too high a rainfall intensity during growth period in Indonesia (Sujono, 2010). These results suggested that the balance and timing of wetting and drying fields highly influence rice yield productivity. Usually, the implementation of conventional method irrigation operations takes 10-15 days based on the availability (on supply). In the study

area, irrigation using the conventional method is still carried out at the survey site, however, the need for irrigation water during the same planting season is not constant (Brouwer & Prins, 1989). Also, it was observed that there are some fields where irrigation water is not sufficiently reached due to the distance from the irrigation canal and small steps between fields or within the fields in the field survey. Based on this, it is considered that these might be a cause of a difference in the contribution of irrigated water amount, and it influences the differences in yield.

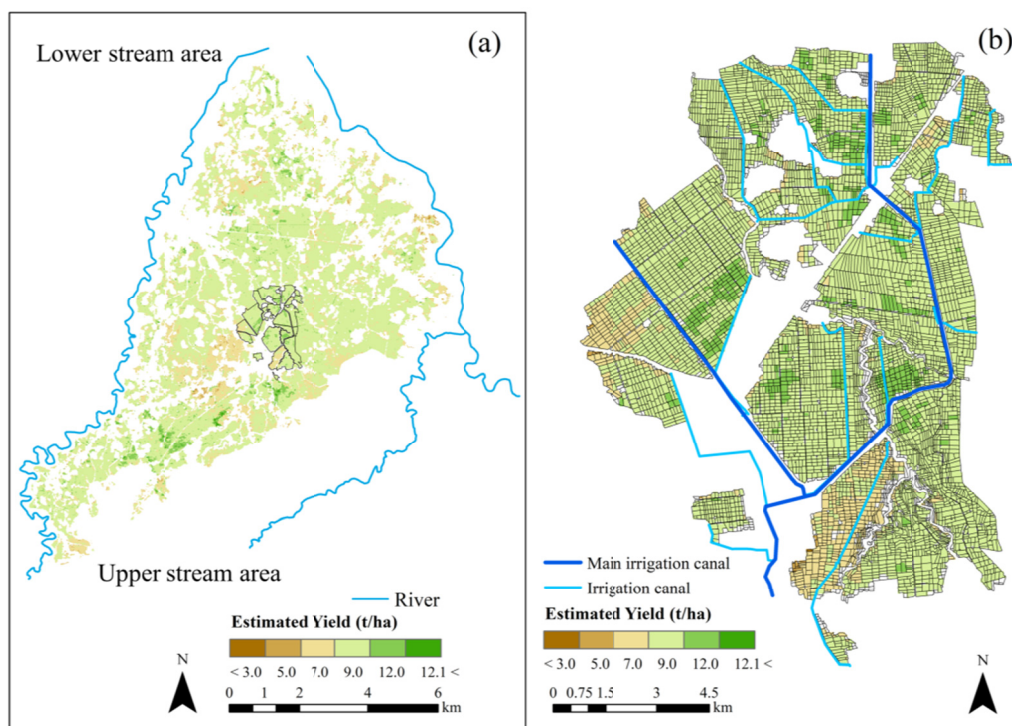


Figure 10. The Mean estimated yield of (a) Cihea, the whole study area; (b) the test sites in the study area located in the middle stream

3.3 Factors of Difference in Annual Yield

Yield estimation results for each year of the study area are shown in Figure 11. Overall, the peak of the estimated yield is at 5~6 t/ha, which is consistent with the range obtained in the field survey (Figure 2). Comparing Figure 11 (a) and (b), the yield tended to be higher in 2019 than in 2018. The water stored as irrigation water in the Cihea Irrigation District is mainly from precipitation. However, it has been already known the amount of water resources in Indonesia fluctuates by season and is distributed unfairly from region to region (Bulsink, Hoekstra, & Booi, 2009; Fulazzaky, 2014). Considering these previous studies, the main reason for the yield difference in our results is presumed that the difference in water content between precipitation and irrigation. To confirm the water condition of paddy fields each year, the distribution of NDWI at 25 days after the heading is shown in Figure 12. In 2018 shown in (a), NDWI tended to be lower than in 2019. And, it was shown that there were many low places where NDWI were around 0.1 to 0.1 from the middle to the lower stream in comparison with 2019, though it was a little high NDWI around 0.3 to 0.4 in the upper stream in 2018. However, the total precipitation from April to September in 2018 was about 461 mm, and that in 2019 was 434 mm, and there was almost no difference in the total precipitation in the growth period of paddy. In addition, 25 days after the heading stage mainly corresponds to July. The precipitation in July from GSMaP was 0 in both years, suggesting that there was little precipitation (Figure 3). Also, solar radiation was extracted from the pixel value corresponding to the upper stream and the lower stream, and the time series change was observed. There was some difference in the watershed (Figure 4). The difference between the lower stream area and the middle stream was 25.26 W/m^2 in 2018, and 21.15 W/m^2 in 2019. Similarly, the difference between the middle stream area and the upper stream area was 20.6 W/m^2 in 2018 and 15.5 W/m^2 in 2019, while the difference between the lower stream area and the upper stream area was 12.5 W/m^2 in 2018 and 13.6 W/m^2 in 2019. Therefore, the moving

average of daily mean solar radiation in each watershed was calculated, and the tendency of each stream was confirmed (Figure 5). The results of the difference in each stream showed that the solar radiation in July, which corresponds to the heading stage or later in the middle and lower streams was higher than in the upper stream in 2018 (Figure 5(a), (b)). On the other hand, solar radiation in the upper stream was a little higher than in the middle stream in 2019 (Figure 5(b)) and the difference was around 15.5 W/m^2 . From these results, it is considered that the total precipitation in the period corresponding to the growth period is almost same for 2 years, however, the solar radiation varies depending on the streams, and the solar radiation in both the middle and the lower reaches tends to be higher than that in the upper reaches in 2018 from June to August, suggesting the possibility that the water obtained by irrigation evaporates and dissipates or irrigation water was not enough for that climate condition. From this result, it was suggested that the water content in the middle and lower streams in 2018 was a little lower than that in 2019, expressed as a difference of about 0.6~1.0 in NDWI, and this might be one of the causes of the low yield in the middle and lower streams. In 2019, solar radiation in the upper stream tended to be high, but the estimated yield did not show a decreasing trend (Figure 11). This is considered because irrigation water was provided enough in the upper stream.

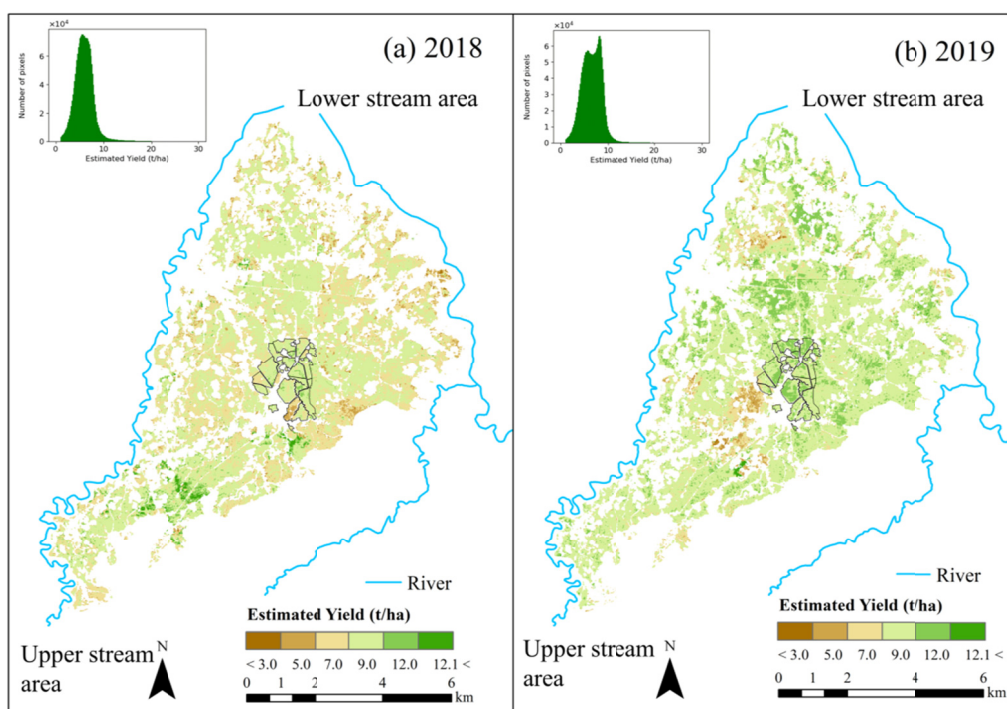


Figure 11. The estimated yield in (a) 2018, (b) 2019 of the whole study area

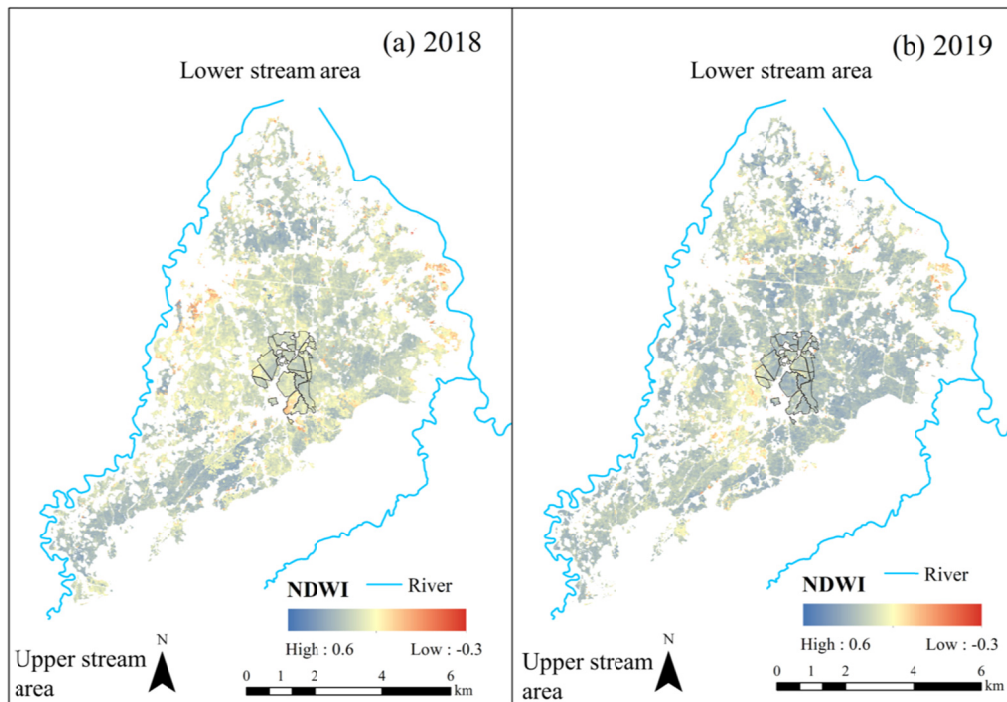


Figure 12. NDWI distribution at 25 days after the estimated heading stage in (a) 2018, (b) 2019 of the whole study area

Figure 13 shows the difference between the estimated yield in 2018 and that in 2019. The larger the positive value shows the higher the yield value in 2018, and the larger the negative value shows the higher the yield value in 2019. A value closer to zero indicates less difference in yield over two years. This figure shows that many regions took the negative value in the lower stream region and the value itself also tended to be large, while the difference for 2 years from the upper stream region to the middle stream region tended to take the value that closes to 0. This suggests that irrigation water supply is relatively stable in the upper stream area, and annual differences due to precipitation and temperature tend to be small. On the other hand, the lower stream area is more sensitive to the effects of weather conditions such as less precipitation and higher temperature. As a result, it is considered that the difference in yield tends to easy to appear in the lower stream.

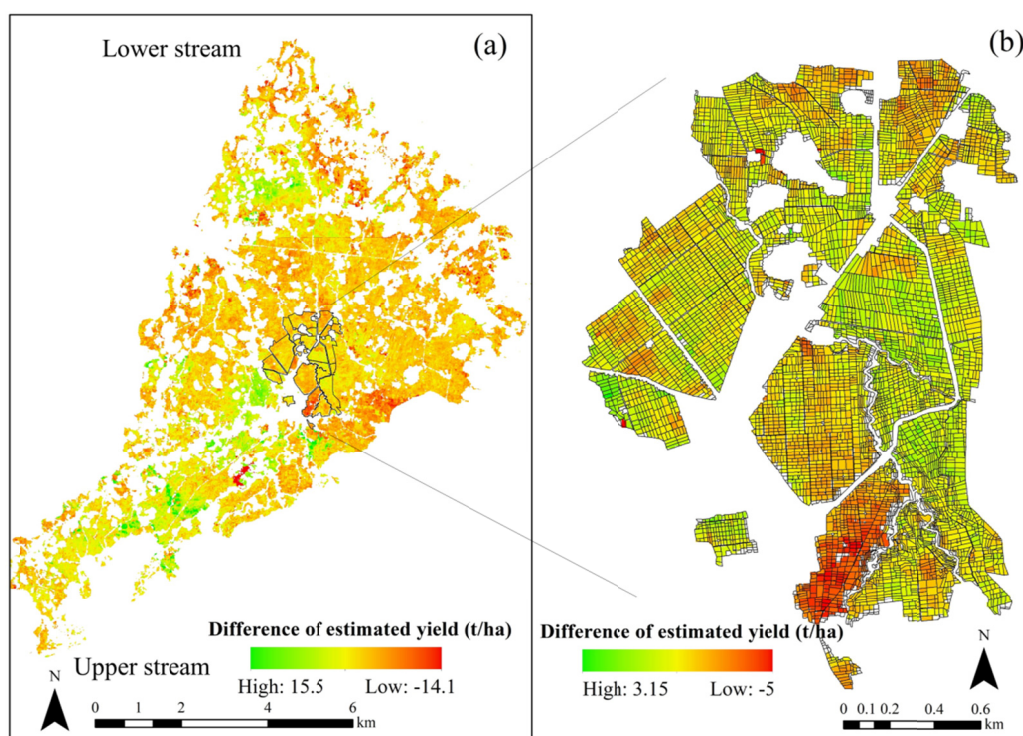


Figure 13. Difference of estimated yield (2018 - 2019) at (a) Cihea; (b) test site

4. Conclusions

Understanding the yield per field is important for the proper management of paddy rice and quantitative damage evaluation. In this study, the spatial variation of rice yield was estimated using the time series SENTINEL-2 satellite data by extracting the growth curve by adjusting the growth stage for each field where the fields with different transplanting dates intermingled. At first, in the field unit, the multiple regression model was created by calculating the reflectance and index every 5 days after the heading stage, and the accuracy of each model was compared and verified. As a result, the red wavelength band and NDWI in the period corresponding to the ripening stage about 25 days after the heading stage were selected as parameters. By using this model equation, it was possible to estimate the yield of the whole study area with an accuracy of coefficient of determination of 0.40 and RMSE of 1.2 t/ha ($p < 0.05$), and it was shown that the remote sensing technique was an effective tool to carry out the continuous yield monitoring in this region in the future. NDWI was selected as one of the parameters which represented environmental conditions, indicating that water is the major limiting factor in the study area. The yield and the NDWI distribution showed differences in the upper stream and lower stream regions of the study area. Since the yield difference by year tends to increase in the lower stream area, it was suggested that the difference by the difference in meteorological conditions tends to increase more in the lower stream area than in the upper stream area. From the above result, it was shown that there was dispersion in the yield by region and year. Therefore, when an insurance system based on yield as one of the evaluation indices is introduced in Indonesia in the future, yield estimation considering the transplanting date and growth stage for each field is necessary.

Acknowledgments

We would like to express our profound gratitude to “The Project for Development and Implementation of New Damage Assessment Process in Agricultural Insurance as Adaptation to Climate Change for Food Security” which is supported by the Japan Science and Technology Agency (JST) and Japan International Cooperation Agency (JICA) as a program of SATREPS (Science and Technology Research Partnership for Sustainable Development). (Grant Number: JPMJSA1604). We would also like to acknowledge the European Space Agency (ESA) for providing the Sentinel-2 satellite datasets, and pest observers who worked together for field surveys in Indonesia.

References

- Ainsworth, E. A. (2008). Rice production in a changing climate: A meta-analysis of responses to elevated carbon dioxide and elevated ozone concentration. *Global Change Biology*, *14*(7), 1642-1650. <https://doi.org/10.1111/j.1365-2486.2008.01594.x>
- Akaike, H. (1998). *Selected Papers of Hirotugu Akaike (Springer Series in Statistics)*. New York, NY: Springer.
- Bessho, K., Date, K., Hayashi, M., Ikeda, A., Imai, T., Inoue, H., ... Yoshida, R. (2016). An introduction to Himawari-8/9—Japan's new-generation geostationary meteorological satellites. *Journal of the Meteorological Society of Japan. Ser. II*, *94*(2), 151-183. <https://doi.org/10.2151/jmsj.2016-009>
- Boor, C. de. (1978). *A Practical Guide to Splines: Applied Mathematical Sciences* (1st ed., p. 27). New York, NY: Springer. <https://doi.org/10.1007/978-1-4612-6333-3>
- Brouwer, C., & Prins, K. (1989). *Irrigation Water Management: Irrigation Scheduling*. Rome, Italy: Director, Publications Division, Food and Agriculture Organization of the United Nations. Retrieved from <https://www.fao.org/3/T7202E/t7202e00.htm#Contents>
- Bulsink, F., Hoekstra, A. Y., & Booij, M. J. (2009). The water footprint of Indonesian provinces related to the consumption of crop products. *Value of Water Research Report Series No. 37*. Delft, the Netherlands: UNESCO-IHE Institute for Water Education. <https://doi.org/10.5194/hessd-6-5115-2009>
- Chen, C., Quilang, E. J. P., Alosnos, E. D., & Finnigan, J. (2011). Rice area mapping, yield, and production forecast for the province of Nueva Ecija using RADARSAT imagery. *Canadian Journal of Remote Sensing*, *37*(1), 1-16. <https://doi.org/10.5589/m11-024>
- Doherty, N. A., & Richter, A. (2002). Moral hazard, basis risk, and gap insurance. *The Journal of Risk and Insurance*, *69*(1), 9-24. <https://doi.org/10.1111/1539-6975.00002>
- Du, H., Fuh, Ru-C. A., Li, J., Corkan, L. A., Lindsey, J. S. (2008). PhotochemCAD[†]: A Computer-Aided Design and Research Tool in Photochemistry. *Photochemistry and Photobiology*, *68*(2), 141-142. <https://doi.org/10.1111/j.1751-1097.1998.tb02480.x>
- Franks, P. J., Adams, M. A., Amthor, J. S., Barbour, M. M., Berry, J. A., Ellsworth, D. S., ... Caemmerer, S. von. (2013). Sensitivity of plants to changing atmospheric CO₂ concentration: from the geological past to the next century. *New Phytologist*, *197*(4), 1077-1094. <https://doi.org/10.1111/nph.12104>
- Fulazzaky, M. A. (2014). Challenges of integrated water resources management in Indonesia. *Water*, *6*(7), 2000-2020. <https://doi.org/10.3390/w6072000>
- Gao, B. C. (1996). NDWI—A normalized difference water index for remote sensing of vegetation liquid water from space. *Remote Sensing of Environment*, *58*(3), 257-266. [https://doi.org/10.1016/S0034-4257\(96\)00067-3](https://doi.org/10.1016/S0034-4257(96)00067-3)
- Hackert, E. C., & Hastenrath, S. (1986). Mechanisms of Java rainfall anomalies. *Monthly Weather Review*, *114*(4), 745-757. [https://doi.org/10.1175/1520-0493\(1986\)114<0745:MOJRA>2.0.CO;2](https://doi.org/10.1175/1520-0493(1986)114<0745:MOJRA>2.0.CO;2)
- Hongo, C., Tsuzawa, T., Tokui, K., & Tamura, E. (2015). Development of damage assessment method of rice crop for agricultural insurance using satellite data. *Journal of Agricultural Science*, *7*(12), 1916-9752. <http://dx.doi.org/10.5539/jas.v7n12p59>
- Kawamura, K., Ikeura, H., Phongchanmaixay, S., & Khanthavong, P. (2018). Canopy hyperspectral sensing of paddy fields at the booting stage and PLS regression can assess grain yield. *Remote Sensing*, *10*(8), 1249. <https://doi.org/10.3390/rs10081249>
- Kobata, T., & Uemuki, N. (2004). High temperatures during the grain-filling period do not reduce the potential grain dry matter increase of rice. *Agronomy Journal*, *96*(2), 406-414. <https://doi.org/10.2134/agronj2004.0406>
- Kubota, T., Aonashi, K., Ushio, T., Shige, S., Takayabu, Y. N., Kachi, M., ... Oki, R. (2020). Global satellite mapping of precipitation (GSMaP) products in the GPM era. *Satellite Precipitation Measurement* (3rd ed.). New York City, United States: Springer. https://doi.org/10.1007/978-3-030-24568-9_20
- Kuwata, K., Mahmood, F., & Shibasaki, R. (2015). Weather index for crop insurance to mitigate basis risk. *2015 IEEE International Geoscience and Remote Sensing Symposium* (pp. 4656-4659). IEEE, Milan, Italy. <https://doi.org/10.1109/IGARSS.2015.7326867>

- Liu, K., Li, Y., Hu, H., Zhou, L., Xiao, X., & Yu, P. (2015). Estimating rice yield based on normalized difference vegetation index at heading stage of different nitrogen application rates in southeast of China. *Journal of Environmental and Agricultural Sciences*, 2(13).
- Liu, W. T., & Kogan, F. (2002). Monitoring Brazilian soybean production using NOAA/AVHRR based vegetation condition indices. *International Journal of Remote Sensing*, 23(6), 1161-1179. <https://doi.org/10.1080/01431160110076126>
- Mahul, O., & Stutley, C. J. (2010). *Government support to agricultural insurance : Challenges and options for developing countries*. World Bank. <https://doi.org/10.1596/978-0-8213-8217-2>
- Manago, N., Hongo, C., Sofue, Y., Sigit, G., & Utoyo, B. (2020). Transplanting date estimation using sentinel-1 satellite data for paddy rice damage assessment in Indonesia. *Agriculture*, 10(12), 625. <https://doi.org/10.3390/agriculture10120625>
- Miranda, M. J., & Gonzalez-Vega, C. (2011). Systemic risk, index insurance, and optimal management of agricultural loan portfolios in developing countries. *American Journal of Agricultural Economics*, 93(2), 399-406. <https://doi.org/10.1093/ajae/aaq109>
- Morton, J. F. (2007). The impact of climate change on smallholder and subsistence agriculture. *Proceedings of the National Academy of Sciences of the United States of America*, 104(50), 19680-19685. <https://doi.org/10.1073/pnas.0701855104>
- Mosleh, M. K., Hassan, Q. K., & Chowdhury, E. H. (2016). Development of a remote sensing-based rice yield forecasting model. *Spanish Journal of Agricultural Research*, 14(3), e0907. <https://doi.org/10.5424/sjar/2016143-8347>
- Naylor, R. L., Battisti, D. S., Vimont, D. J., Falcon, W. P., & Burke, M. B. (2007). Assessing risks of climate variability and climate change for Indonesian rice agriculture. *Proceedings of the National Academy of Sciences of the United States of America*, 104(19), 7752-7757. <https://doi.org/10.1073/pnas.0701825104>
- O'Brien, K., Leichenko, R., Kelkar, U., Venema, H., Aandahl, G., Tompkins, H., ... West, J. (2004). Mapping vulnerability to multiple stressors: climate change and globalization in India. *Global Environmental Change*, 14(4), 303-313. <https://doi.org/10.1016/j.gloenvcha.2004.01.001>
- Panuju, D. R., Mizuno, K., & Trisasonko, B. H. (2013). The dynamics of rice production in Indonesia 1961-2009. *Journal of the Saudi Society of Agricultural Sciences*, 12(1), 27-37. <https://doi.org/10.1016/j.jssas.2012.05.002>
- Santosa, M., & Suryanto, A. (2015). The growth and yield of paddy Ciherang planted in dry and wet season and fertilized with organic and inorganic fertilizers. *Journal of Agricultural Science*, 37(1), 24-29. <http://doi.org/10.17503/agrivita.v37i1.251>
- Song, Y., Wang, C., Linderholm, H. W., Fu, Y., Cai, W., Xu, J., ... Chen, D. (2022). The negative impact of increasing temperatures on rice yields in southern China. *Science of the Total Environment*, 820(10), 153262. <https://doi.org/10.1016/j.scitotenv.2022.153262>
- Soriano-González, J., Angelats, E., Martínez-Eixarch, M., & Alcaraz, C. (2022). Monitoring rice crop and yield estimation with Sentinel-2 data. *Field Crops Research*, 281(15). <https://doi.org/10.1016/j.fcr.2022.108507>
- Sujono, J. (2010). Flood reduction function of paddy rice fields under different water saving irrigation techniques. *Journal of Water Resource and Protection*, 2(6), 555-559. <https://doi.org/10.4236/jwarp.2010.26063>
- Swami, S. (2017). *Effect of solar radiation in crop production: Natural Resource Management for Climate Smart Sustainable Agriculture*. New Delhi, India: Soil Conservation Society.
- Takenaka, H., Nakajima, T. Y., Higurashi, A., Higuchi, A., Takamura, T., Pinker, R. T., Nakajima, T. (2011). Estimation of solar radiation using a neural network based on radiative transfer. *Journal of Geophysical Research Atmosphere*, 116(D8), D08251. <https://doi.org/10.1029/2009JD013337>
- Yazd, S. D., Wheeler, S. A., & Zuo, A. (2020). Understanding the impacts of water scarcity and socio-economic demographics on farmer mental health in the Murray-Darling Basin. *Ecological Economics*, 169. <https://doi.org/10.1016/j.ecolecon.2019.106564>
- Yuliawan, T., & Handoko, I. (2016). The Effect of Temperature Rise to Rice Crop Yield in Indonesia uses Shierary Rice Model with Geographical Information System (GIS) Feature. *Procedia Environmental Sciences*, 33, 214-220. <https://doi.org/10.1016/j.proenv.2016.03.072>

Zaman, N. K., Abdullah, M. Y., Othman, S., & Zaman, N. K. (2018). Growth and Physiological Performance of Aerobic and Lowland Rice as Affected by Water Stress at Selected Growth Stages. *Rice Science*, 25(2), 82-93. <https://doi.org/10.1016/j.rsci.2018.02.001>

Copyrights

Copyright for this article is retained by the author(s), with first publication rights granted to the journal.

This is an open-access article distributed under the terms and conditions of the Creative Commons Attribution license (<http://creativecommons.org/licenses/by/4.0/>).